

The Biomarker TCONS_00016233 Drives Septic AKI by Targeting the miR-22-3p/AIFM1 Signaling Axis

Pan Zhang,^{1,2,8} Lei Yi,^{1,2,3,8} Siyuan Qu,⁵ Jinzhong Dai,^{1,2} Xiaozhou Li,^{1,2} Bohao Liu,^{1,2} Huiling Li,⁴ Kai Ai,³ Peilin Zheng,⁶ Shuangfa Qiu,^{1,2} Yijian Li,³ Yinhuai Wang,³ Xudong Xiang,^{1,2} Xiangping Chai,^{1,2} Zheng Dong,^{5,7} and Dongshan Zhang^{1,2}

¹Department of Emergency Medicine, Second Xiangya Hospital, Central South University, Changsha, Hunan, People's Republic of China; ²Emergency Medicine and Difficult Diseases Institute, Second Xiangya Hospital, Central South University, Changsha, Hunan, People's Republic of China; ³Department of Urology, Second Xiangya Hospital, Central South University, Changsha, Hunan, People's Republic of China; ⁴Department of Ophthalmology, Second Xiangya Hospital, Central South University, Changsha, Hunan, People's Republic of China; ⁵Department of Nephrology, Second Xiangya Hospital, Central South University, Changsha, Hunan, People's Republic of China; ⁶Department of Endocrinology, Shenzhen People's Hospital, The Second Clinical Medical College of Jinan University, The First Affiliated Hospital of Southern University of Science and Technology, Shenzhen, China; ⁷Department of Cellular Biology and Anatomy, Medical College of Georgia at Georgia Regents University and Charlie Norwood VA Medical Center, Augusta, GA, USA

The prediction of mortality for septic acute kidney injury (AKI) has been assessed by a number of potential biomarkers, including long noncoding RNAs (lncRNAs). However, the validation of lncRNAs as biomarkers, particularly for the early stages of septic AKI, is still warranted. Our results indicate that the lncRNA TCONS_00016233 is upregulated in plasma of sepsis-associated non-AKI and AKI patients, but a higher cutoff threshold (9.5×10^5 , copy number) provided a sensitivity of 71.9% and specificity of 89.6% for the detection of AKI. The plasma TCONS_00016233 was highly correlated with serum creatinine, tissue inhibitor metalloproteinase-2 (TIMP-2), insulin-like growth factor binding protein-7 (IGFBP7), interleukin-1 β (IL-1 β), tumor necrosis factor α (TNF- α), C-reactive protein (CRP), and urinary TCONS_00016233. Lipopolysaccharide (LPS) induced the expression of lncRNA TCONS_00016233 via the Toll-like receptor 4 (TLR4)/p38 mitogen-activated protein kinase (MAPK) signal pathway in human renal tubular epithelial (HK-2) cells. Furthermore, TCONS_00016233 mediates the LPS-induced HK-2 cell apoptosis and the expression of IL-1 β and TNF- α . Mechanistically, TCONS_00016233 acts as a competing endogenous RNA (ceRNA) to prevent microRNA (miR)-22-3p-mediated downregulation of the apoptosis-inducing factor mitochondrion-associated 1 (AIFM1). Finally, overexpression of TCONS_00016233 is capable of aggravating the LPS- and cecal ligation and puncture (CLP)-induced septic AKI by targeting the miR-22-3p/AIFM1 axis. Taken together, our data indicate that TCONS_00016233 may serve as an early diagnosis marker for the septic AKI, possibly acting as a novel therapeutic target for septic AKI.

INTRODUCTION

Sepsis is an aggressive and life-threatening medical condition caused by a dysregulated host response to severe infection. Acute kidney injury (AKI) is one of the most serious complications of sepsis, and it occurs

in about 50%–60% of the affected patients.¹ Several studies indicate that early diagnosis may provide better opportunities for a timely intervention.^{2,3} Hence, the development of reliable biomarkers is very important for the early diagnosis of septic AKI. In the past decades, several protein biomarkers, including the soluble form of the triggering receptor expressed on myeloid cells 1 (TREM-1), tissue inhibitor metalloproteinase-2 (TIMP-2), insulin-like growth factor binding protein-7 (IGFBP7), kidney injury molecule-1 (KIM-1), netrin-1, and neutrophil gelatinase-associated lipocalin (NGAL), have demonstrated some diagnostic value for septic AKI.^{4–9} More recently, long noncoding RNAs (lncRNAs) have been recognized as a new, promising class of biomarkers in the diagnosis of various human diseases.^{10,11}

lncRNAs compose a group of RNA molecules (longer than 200 nt) that can act as a competing endogenous RNA (ceRNA) to control microRNA (miRNA) activity.¹² Interestingly, some studies have suggested that circulating lncRNAs could be regarded as a biomarker for sepsis-related conditions.^{13,14} Still, it is not fully clear whether circulating lncRNAs could be utilized as putative early biomarkers of septic AKI.

In the current study, we have discovered that circulating and urinary lncRNA TCONS_00016233 is a diagnosis biomarker of septic AKI patients. *In vitro* assays suggest that induction of TCONS_00016233 can regulate apoptosis-inducing factor mitochondrion-associated 1 (AIFM1) expression to further increase renal cell apoptosis via sponging miRNA (miR)-22-3p. Finally, overexpression of

Received 25 October 2019; accepted 5 December 2019;
<https://doi.org/10.1016/j.omtn.2019.12.037>.

⁸These authors contributed equally to this work.

Correspondence: Dongshan Zhang, MD, Department of Emergency Medicine, Second Xiangya Hospital, Central South University, Changsha, Hunan 410011, People's Republic of China.

E-mail: dongshanzhang@csu.edu.cn



Table 1. Summary of Baseline Physiology and Laboratory Values

Characteristic	Septic AKI (n = 15)	Septic Non-AKI (n = 15)	p Value
Age (years) (mean [SD])	62.13 (15.72)	52.73 (18.68)	0.147
Male sex (%)	60.0	40.0	0.713
Temperature (°C) (median [IQR])	36.8 (36.2–38)	38.1 (37.8–38.5)	0.005
Respiratory rate (times/min) (mean [SD])	23.6 (5.44)	26.33 (6.46)	0.22
Heart rate (beats/min) (mean [SD])	110.2 (20.68)	113.87 (10.78)	0.548
MAP (mmHg) (mean [SD])	78.42 (18.93)	81.22 (15.47)	0.661
PaO ₂ (mmHg) (mean [SD])	92.13 (35.40)	87.51 (43.98)	0.75
White cell count (10 ⁹ /mL) (mean [SD])	13.65 (3.06)	14.01 (1.58)	0.692
Platelets (10 ⁹ /mL) (mean [SD])	75.47 (20.01)	93.33 (31.05)	0.073
C-reactive protein (mg/L) (mean [SD])	97.52 (26.47)	110.97 (16.77)	0.108
Procalcitonin (ng/mL) (mean [SD])	6.30 (3.25)	4.71 (1.90)	0.113
Lactate (mM) (median [IQR])	2.1 (1.2–5.7)	1.3 (1.0–3.6)	0.161
Blood urea nitrogen (mM) (mean [SD])	20.89 (4.83)	7.05 (2.33)	<0.001
Serum creatinine (μM) (mean [SD])	229.03 (53.48)	71.17 (24.66)	<0.001
Activated partial thromboplastin time (s) (mean [SD])	49.22 (9.05)	46.65 (9.25)	0.448
Alanine aminotransferase (U/L) (mean [SD])	83.61 (23.85)	100.53 (35.76)	0.138
Total bilirubin (μM) (mean [SD])	37.10 (9.58)	31.96 (18.10)	0.339
Blood glucose (mM) (mean [SD])	8.94 (2.47)	6.96 (2.06)	0.024
SOFA score (mean [SD])	7.00 (1.36)	6.53 (1.30)	0.346

IQR, interquartile range; MAP, mean arterial pressure; PaO₂, partial pressure of oxygen; SOFA, sequential organ failure assessment.

TCONS_00016233 aggravated the lipopolysaccharide (LPS)- and cecal ligation and puncture (CLP)-induced septic AKI by targeting the miR-22-3p/AIFM1 axis. Collectively, our data indicate that TCONS_00016233 may not only serve as an early diagnosis marker but also as a mediator of septic AKI progression.

RESULTS

Plasma TCONS_00016233 Is Induced in Septic AKI and Non-AKI Patients

To investigate the expression of circulating lncRNAs, total RNA was, respectively, isolated from septic AKI (n = 15) and non-AKI (n = 15) patients and from healthy, age-matched controls (n = 15). RNA samples, from each respective group, were then mixed to perform a lncRNA chip assay. The clinical characteristics of the whole cohort of AKI patients (n = 15) are shown in Table 1. A representative lncRNA heatmap is shown in (Figure 1A). A total of 881 and 332 lncRNAs were upregulated (>2-fold change) in septic AKI or non-AKI versus control groups, respectively (Figure 1B; Tables S1 and S2). A total of 203 lncRNAs were

co-upregulated in both septic AKI and non-AKI when compared to the control group (Figure 1B; Table S3). As shown in Figure 1C, eleven co-upregulated lncRNAs increase by more than 50-fold in septic AKI versus the control group. Among these, TCONS_00016233 was the highest co-upregulated lncRNAs (218- and 98-fold change in septic AKI and non-AKI versus control, respectively). Quantitative real-time PCR (qRT-PCR) analysis confirmed that TCONS_00016233 was indeed induced in septic AKI and non-AKI patients when compared to healthy controls (2.25- and 1.3-fold change in septic AKI and non-AKI versus control, respectively; Figure 1D). Taken together, our data indicate an increased detection of TCONS_00016233 in the plasma of septic AKI and non-AKI patients.

TCONS_00016233 Was a Marker of AKI

To assess whether TCONS_00016233 in the plasma could be considered as a diagnosis marker in septic AKI patients, we expanded the sample size to septic patients with AKI (n = 96), non-AKI (n = 96), and age-matched healthy individuals (n = 30) and further examined TCONS_00016233 expression. The clinical characteristics of the whole cohort of septic AKI and non-AKI patients (n = 96) are shown in Table 2. Absolute real-time PCR analysis indicated that the copy number of plasma TCONS_00016233 mildly increased in septic non-AKI patients when compared to the controls (Figure 2A). Interestingly, a more prominent, increased TCONS_00016233 expression was noticed in septic AKI patients (Figure 2A). To assess the diagnostic value of TCONS_00016233, receiver operating characteristic (ROC) curves were generated. As shown in Figure 2B, the area under the ROC curve (AUC) was found to be 0.894 (95% confidence interval, 0.852–0.936), with a sensitivity of 71.9% and specificity of 89.6%, at a higher cutoff value of 9.5×10^5 copy number. TCONS_00016233 levels increased proportionally to the Kidney Disease: Improving Global Outcomes (KDIGO) staging of the patients (Figure 2C). The Spearman correlation coefficient indicated that the levels of plasma TCONS_00016233 were highly correlated with the expression of serum creatinine, TIMP-2, IGFBP7, C-reactive protein (CRP), interleukin-1 β (IL-1 β), and tumor necrosis factor α (TNF- α) (r = 0.769, 0.302, 0.590, 0.017, 0.181, and 0.311, respectively, p < 0.001; Figures 2D–2F and 2I–2K). Finally, we verified that the increased levels of urinary TCONS_00016233 were consistent and highly correlated with the plasma TCONS_00016233 (r = 0.638, p < 0.001; Figures 2G and 2H). These data reiterate the potential use of TCONS_00016233 as an early marker for AKI.

TCONS_00016233 Is Induced in LPS-Treated Human Renal HK-2 Cells via TLR4/p38MAPK Axis

To verify whether major sepsis-related components could drive the induction of TCONS_00016233 in kidney cells, we treated an immortalized proximal human renal tubular epithelial cell line (HK-2) with bacterial lipopolysaccharides (LPS) and detected TCONS_00016233 by fluorescent *in situ* hybridization (FISH) analysis. The data indicate that TCONS_00016233 is located in the cytoplasm of HK-2 cells (Figure 3A). Moreover, qRT-PCR results show that TCONS_00016233 expression is induced after 12 h and 24 h of LPS treatment (Figure 3B). Furthermore, Toll-like receptor 4 (TLR4) small interfering RNA (siRNA) markedly suppressed the activation of p38 mitogen-

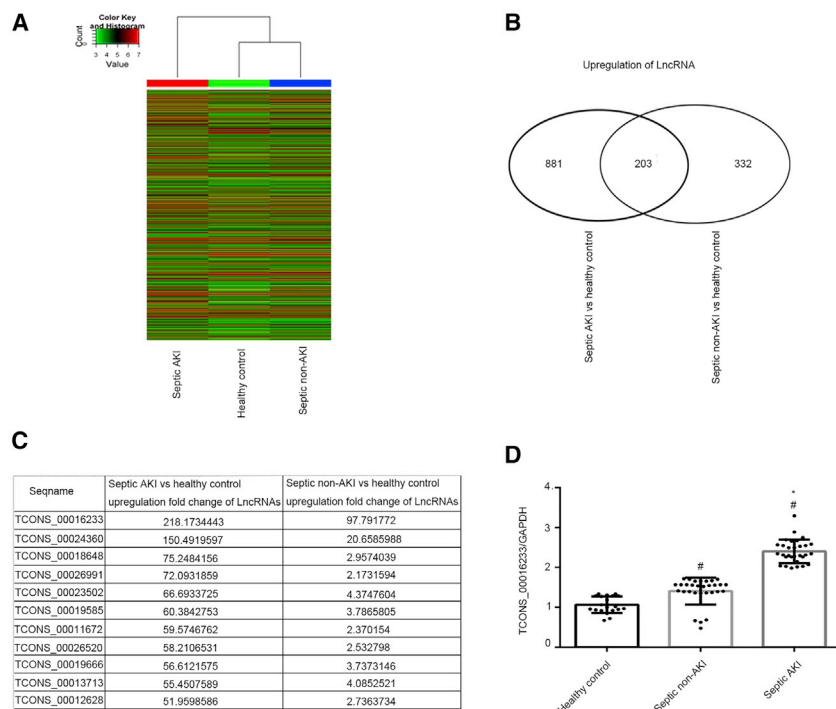


Figure 1. The TCONS_00016233 Was Increased in Septic AKI and Non-AKI Patients

(A) The lncRNA heatmap. (B) The changes amount of co-upregulation lncRNAs between (more than 2-fold changes) septic AKI or septic non-AKI versus control. (C) The name and fold changes of co-upregulation lncRNAs (more than 50-fold changes) between them. (D) qRT-PCR analysis of the expression levels of TCONS_00016233. Data are expressed as mean \pm SD (n = 15 or 30). #p < 0.05, septic non-AKI or septic AKI versus control group; *p < 0.05, septic AKI group versus septic non-AKI.

TCONS_00016233 expression can be further enhanced by TCONS_00016233 overexpression in HK-2 cells (Figure 5A). Moreover, FCM results reiterated that TCONS_00016233 overexpression markedly aggravates LPS-induced renal cell apoptosis in HK-2 cells (Figures 5B and 5C). Consistently, immunoblot analysis demonstrated that TCONS_00016233 overexpression can markedly augment LPS-caused accumulation of the cleaved caspase-3 protein (Figures 5D and 5E). Finally, overexpression of TCONS_00016233 enhances LPS-induced expression of IL-1 β and TNF- α (Figures 5F–5I). These data agree with previous knockdown experiments, supporting the notion that TCONS_00016233 acts as an apoptotic and inflammation inducer in LPS-treated HK-2 cells.

TCONS_00016233 Inhibited the Expression and Activity of miR-22-3p

Typically, lncRNAs act as competitive endogenous RNAs (ceRNAs) and sponge miRNAs. To examine which miRNAs would be potentially modulated by TCONS_00016233, we performed a target-prediction analysis *in silico* (using RegRNA 2.0 software). The prediction results indicated that the 3' sequence of TCONS_00016233 contained an miR-22-3p binding site (Figure 6A). Functional analysis, based on a luciferase reporter gene assay, indicates that a miR-22-3p mimic can markedly suppress the luciferase activity of TCONS_00016233-wild-type (WT) but not TCONS_00016233-mutant (MUT) (Figure 6B). Indeed, colocalization analysis indicated that TCONS_00016233 may interact with miR-22-3p in the cytosolic compartment of both untreated and LPS-stimulated HK-2 cells (Figure 6C). Furthermore, in sham mice, the FISH data only detected the expression of miR-22-3p but not TCONS_00016233, which confirmed that high conservation of TCONS_00016233 is not expressed in mice. In *in vivo* injection of TCONS_00016233 expressing vector mice, FISH analysis detected that exogenous TCONS_00016233 interacts with endogenous miR-22-3p in the cytosol of tubular kidney cells of LPS- or CLP-induced AKI in mice (Figure 6D). LPS-mediated expression inhibition of miR-22-3p is reversed by TCONS_00016233 knockdown, but contrarily, TCONS_00016233 overexpression reinforced this effect (Figures 6E and 6F). Taken together, these data demonstrate that miR-22-3p is a direct target of TCONS_00016233.

activated protein kinase (MAPK) and the expression of TCONS_00016233 (Figures 3C–3E). In addition, inactivation of p38MAPK reduced the expression of TCONS_00016233 (Figures 3F–3H). Finally, the effect of TLR4 siRNA on LPS-induced expression of TCONS_00016233 was reversed by the p38MAPK agonist. Therefore, LPS may lead the expression of TCONS_00016233 in kidney cells via the TLR4/p38MAPK axis.

Knockdown of TCONS_00016233 Expression Ameliorated LPS-Induced Renal Cell Apoptosis

Apoptosis has an important role in septic AKI.¹⁵ So, we investigated whether TCONS_00016233 might be involved in LPS-induced renal cell apoptosis. qRT-PCR analysis has showed that LPS-induced TCONS_00016233 expression in HK-2 cells was markedly suppressed by transient gene silencing using TCONS_00016233 siRNA (Figure 4A). Additionally, flow cytometry (FCM) results indicate that TCONS_00016233 gene silencing notably inhibits the LPS-induced apoptosis of siRNA-transfected HK-2 cells (Figures 4B and 4C). Consistently, immunoblot analysis shows that the siRNA-mediated TCONS_00016233 knockdown significantly reduced LPS-induced accumulation of cleaved caspase-3 (Figures 4D and 4E). These data suggest that TCONS_00016233 can mediate LPS-induced apoptosis *in vitro*.

Overexpression of TCONS_00016233 Aggravates LPS-Induced Renal Cell Apoptosis and the Expression of IL-1 β and TNF- α

To verify whether increased TCONS_00016233 levels would also impact LPS-induced apoptosis *in vitro*, a TCONS_00016233 expression vector was transfected into HK-2 cells for further functional analyses. qRT-PCR analysis showed that LPS-induced

Table 2. Summary of Baseline Physiology and Laboratory Values

Characteristic	Septic AKI (n = 96)	Septic Non-AKI (n = 96)	p Value
Age (years) (mean [SD])	59.53 (15.66)	53.39 (16.55)	0.009
Male sex (%)	57.30	47.90	0.193
Temperature (°C) (median [IQR])	36.9 (36.5–37.7)	37.45 (36.6–38.3)	0.013
Respiratory rate (times/min) (mean [SD])	23.91 (6.047)	23.01 (5.224)	0.273
Heart rate (beats/min) (mean [SD])	101.95 (23.553)	99.91 (19.851)	0.517
MAP (mmHg) (mean [SD])	86.65 (23.22)	84.85 (15.69)	0.53
PaO ₂ (mmHg) (mean [SD])	89.42 (26.08)	88.47 (32.69)	0.824
White cell count (10 ⁹ /mL) (mean [SD])	15.59 (10.46)	13.98 (7.70)	0.227
Platelets (10 ⁹ /mL) (mean [SD])	132.04 (95.03)	178.95 (129.327)	0.005
C-reactive protein (mg/L) (mean [SD])	95.07 (104.05)	101.77 (90.08)	0.653
Procalcitonin (ng/mL) (mean [SD])	27.39 (37.74)	8.48 (17.52)	<0.001
Lactate (mM) (median [IQR])	1.5 (1.1–3.4)	1.2 (0.6–2.5)	0.009
Blood urea nitrogen (mM) (mean [SD])	21.99 (9.58)	9.96 (30.17)	<0.001
Serum creatinine (μM) (mean [SD])	343.23 (224.12)	71.00 (24.60)	<0.001
Activated partial thromboplastin time (s) (mean [SD])	51.08 (22.10)	43.42 (10.49)	0.058
Alanine aminotransferase (U/L) (mean [SD])	213.53 (503.67)	89.14 (120.7)	0.02
Total bilirubin (μM) (mean [SD])	39.83 (64.66)	24.23 (30.25)	0.034
Blood glucose (mM) (mean [SD])	8.73 (4.62)	8.76 (6.35)	0.962
SOFA score (mean [SD])	7.8 (3.54)	4.75 (2.33)	<0.001

miR-22-3p Mimic Attenuates LPS-Induced Renal Cell Apoptosis

It has been demonstrated that miR-22-3p has an anti-apoptosis role in several tumor cells lines.¹⁶ However, the role of miR-22-3p in LPS-induced renal cell apoptosis remains unclear. qRT-PCR results indicate that the miR-22-3p mimic can, in fact, increase the levels of miR-22-3p in HK-2 cells, treated or not with LPS (Figure 7A). FCM results indicate that the miR-22-3p mimic suppresses LPS-induced renal cell apoptosis in HK-2 cells (Figures 7B and 7C). Consistently, immunoblot assays demonstrated that the miR-22-3p mimic significantly inhibits LPS-induced accumulation of the cleaved caspase-3 (Figures 7D and 7E). Therefore, these results indicate that miR-22-3p can protect HK-2 cells against LPS-induced apoptosis.

AIFM1 Is a Direct miR-22-3p Target Gene and Mediates LPS-Induced Renal Cell Apoptosis

Recent studies have reported that apoptosis-inducing factor mitochondrion-associated 1 (AIFM1) protein can stimulate apoptosis

in hepatoma cells.¹⁷ By performing computational analysis (using the miRBase database), we have predicted that AIFM1 is a putative miR-22-3p target gene (Figure 8A). In fact, reporter assays here demonstrate that the miR-22-3p mimic suppresses the luciferase activity of AIFM1-WT but not AIFM1-MUT (Figure 8B). qRT-PCR and immunoblot results show that the miR-22-3p mimic significantly decreases AIFM1 mRNA and protein levels (Figures 8C and 8D). FCM results indicate that AIFM1 knockdown markedly suppresses LPS-induced renal cell apoptosis in HK-2 cells (Figures 8E and 8F). Immunoblot results demonstrated that silencing of AIFM1 expression can notably suppress LPS-induced accumulation of the cleaved caspase-3 (Figures 8G and 8H). Altogether, these data demonstrate that AIFM1 might be a direct target gene of miR-22-3p.

miR-22-3p Mediates the Proapoptosis Effects of TCONS_00016233

We further evaluated whether miR-22-3p could mediate the proapoptotic effects of TCONS_00016233 in LPS-treated HK-2 cells. Both transfection efficiency of TCONS_00016233 siRNA and treatment with the miR-22-3p inhibitor *in vitro* were validated by qRT-PCR (Figures 9A and 9B). FCM analysis demonstrated that TCONS_00016233 knockdown is able to attenuate LPS-induced renal cell apoptosis, and this effect could be reversed with miR-22-3p inhibitor treatment (Figures 9C and 9D). Immunoblot analysis of cleaved caspase-3 and AIFM1 further supported the FCM findings and confirmed a potential apoptosis-related mechanism (Figures 9E and 9F). These data further confirm that TCONS_00016233 mediated the LPS-induced renal cell apoptosis by targeting the miR-22-3p/AIFM1 axis.

TCONS_00016233 Overexpression Aggravates LPS-Induced AKI *In Vivo* by Targeting the miR-22-3p/AIFM1 Axis

To better elucidate the function of TCONS_00016233 in septic AKI, C57BL/6J mice were pretreated with the TCONS_00016233-expressing vector via tail vein for 12 h and then injected with LPS for a further 24 h. The renal function results indicated that overexpression of TCONS_00016233 markedly increases the LPS-induced levels of blood urea nitrogen (BUN) and creatinine (Figures 10A and 10B). Hematoxylin and eosin (H&E) staining indicated that overexpression of TCONS_00016233 can enhance LPS-induced tubular damage in the cortex and outer stripe of outer medulla (OSOM) of mice kidney (Figures 10C and 10D). The FISH analysis demonstrated that TCONS_00016233 was mainly expressed in the tubular cells of kidney after LPS with injection of TCONS_00016233 (Figure S4A). These observations were quantified as tubular damage scores (Figures 10F and 10G). TUNEL staining indicated that TCONS_00016233 overexpression enhances the tubular cell apoptosis caused by LPS (Figures 10E–10H). qRT-PCR was performed to validate the delivery of ectopic TCONS_00016233 into the mice kidney, with or without the LPS treatment group (Figure S1A). This overexpression further enhanced the LPS-induced suppression of miR-22-3p (Figure S1B). The expression of cleaved caspase-3 and AIFM1 was induced by LPS, which was further synergized by TCONS_00016233

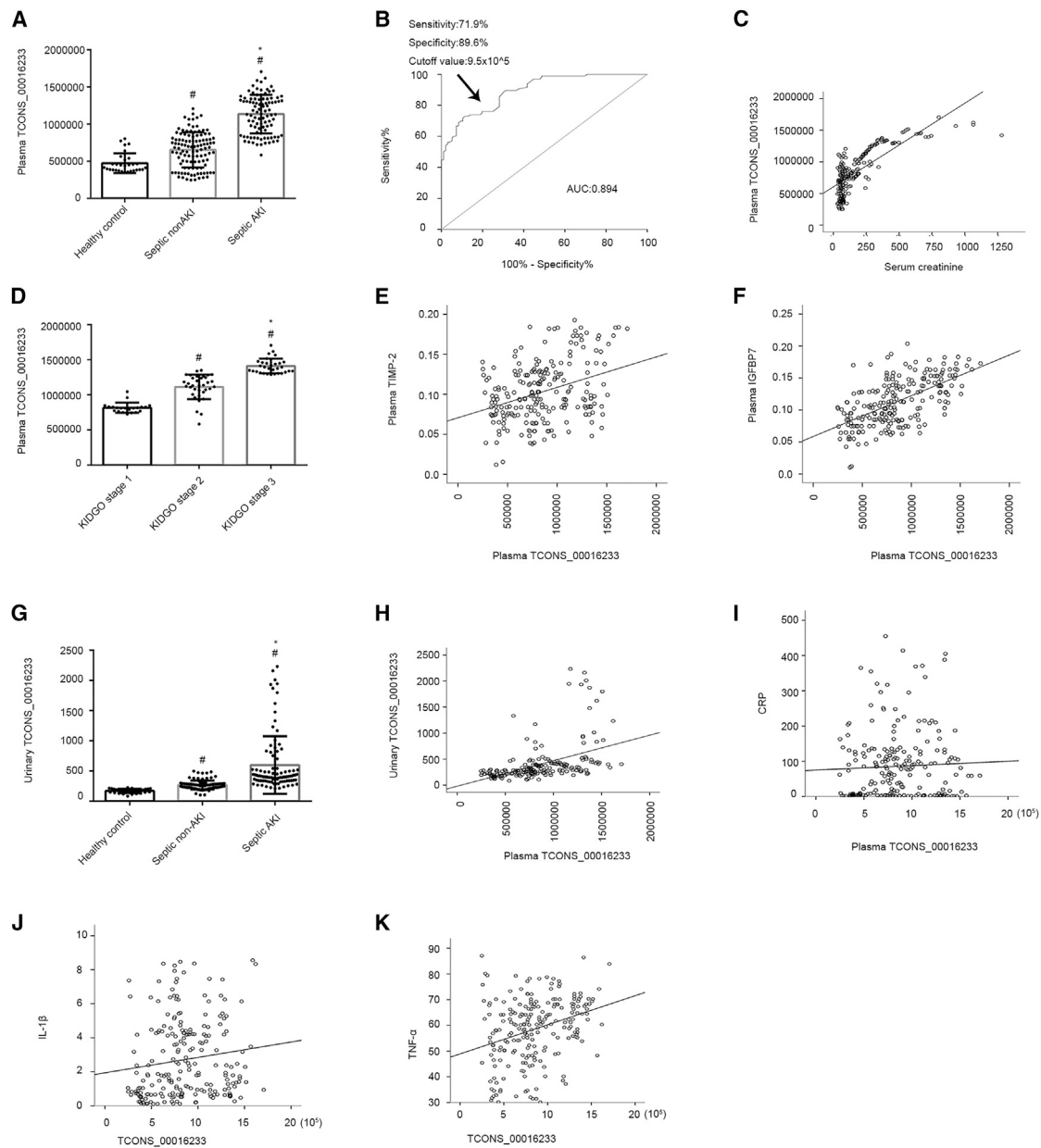


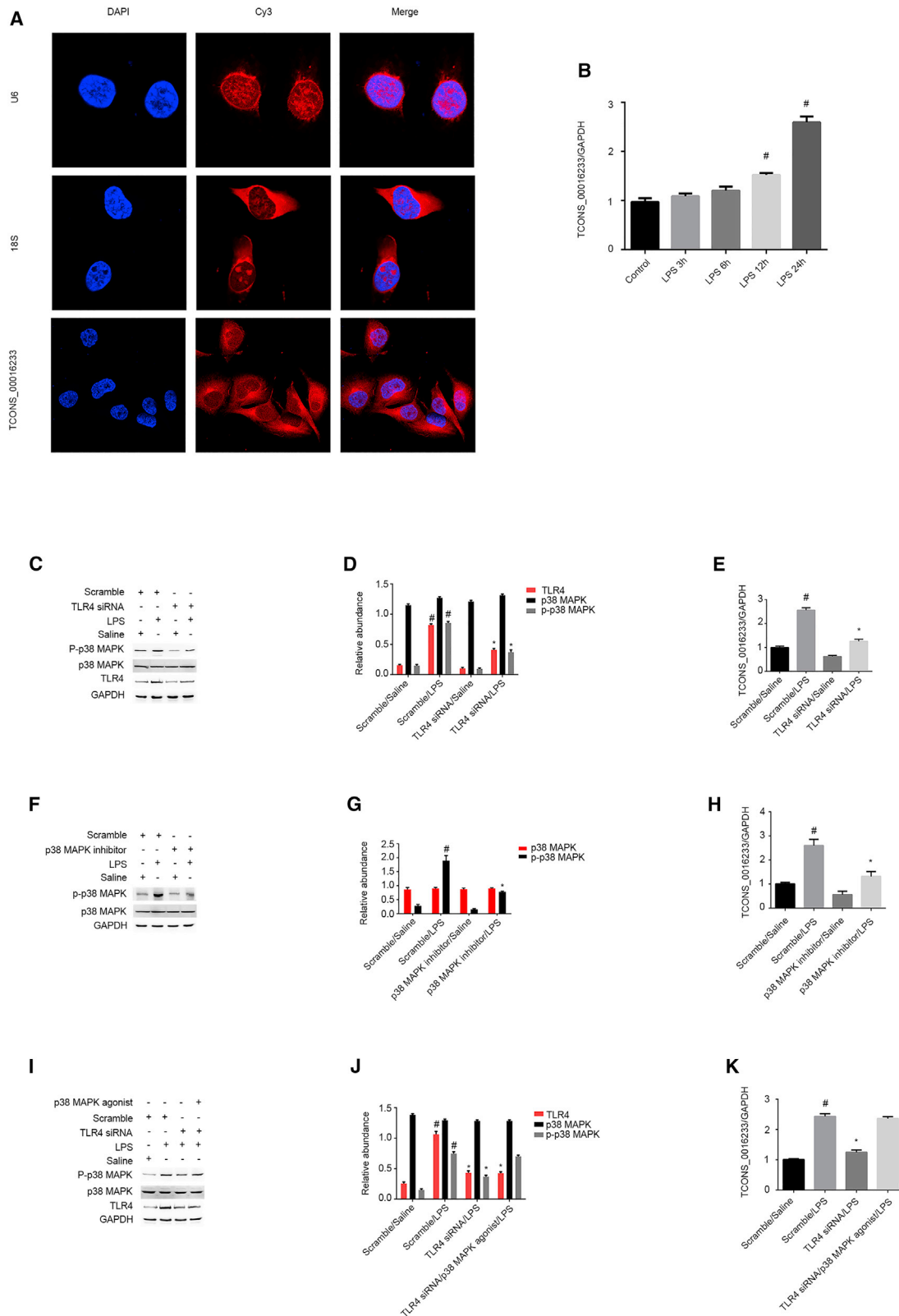
Figure 2. The TCONS_00016233 Was a Diagnosis Marker of AKI

(A) Absolute real-time PCR analysis of plasma TCONS_00016233. (B) Area under receiver-operator characteristic curve for diagnosis of septic AKI versus septic non-AKI for a peak plasma TCONS_00016233. (C) The expression of TCONS_00016233 in different stages of septic AKI. (D–F and I–K) The correlation analysis of TCONS_00016233 with creatinine (D), TIMP-2 (E), IGFBP7 (F), CRP (I), IL-1 β (J), and TNF- α (K). (G) Absolute real-time PCR analysis of urinary TCONS_00016233. (H) The correlation analysis of plasma and urinary TCONS_00016233. Data are expressed as mean \pm SD (n = 96). #p < 0.05, septic non-AKI or septic AKI versus control group or stages III or II of septic AKI versus stage I; *p < 0.05, septic AKI group versus septic non-AKI or stage III of septic AKI versus stage II.

overexpression (Figures S1C and S1D). Finally, the immunoblot and qRT-PCR analysis demonstrated that overexpression of TCONS_00016233 enhanced LPS-induced expression of IL-1 β and TNF- α (Figures S1E–S1H). These data support the hypothesis that TCONS_00016233 is involved in the progression of LPS-induced AKI.

TCONS_00016233 Overexpression Exacerbates CLP-Induced AKI *In Vivo* by Targeting the miR-22-3p/AIFM1 Axis

To confirm the findings of LPS-induced AKI *in vivo*, an additional mouse model was used. C57BL/6J mice were preinjected with the TCONS_00016233 plasmid via tail vein for 12 h and then subjected to CLP for 18 h. A biochemical evaluation of renal function



(legend on next page)

indicated that TCONS_00016233 overexpression largely increased CLP-induced levels of both BUN and creatinine (Figures S2A and S2B). H&E staining indicated that overexpression of TCONS_00016233 also exacerbated CLP-induced tubular damage in the cortex and OSOM of mice kidney (Figures S2C and S2D), which was consistent with the tubular damage scores (Figures S2F and S2G). TUNEL staining results indicated that overexpression of TCONS_00016233 increased CLP-induced tubular cell apoptosis (Figures S2E–S2H). The FISH analysis demonstrated that TCONS_00016233 was mainly expressed in the tubular cells of the kidney after CLP with injection of TCONS_00016233 (Figure S4B). The qRT-PCR data indicated that transfection of TCONS_00016233 can enhance the CLP-mediated suppression of miR-22-3p (Figures S3A and S3B). Immunoblot analysis showed that CLP can upregulate the expression levels of cleaved caspase-3 and AIFM1, which were further enhanced by TCONS_00016233 overexpression (Figures S3C and S3D). Finally, the immunoblot and qRT-PCR analysis demonstrated that overexpression of TCONS_00016233 enhanced CLP-induced expression of IL-1 β and TNF- α (Figures S1E–S1H). These conclusive data further confirmed that TCONS_00016233 can mediate the CLP-dependent AKI progression.

DISCUSSION

Here, we demonstrate for the first time that TCONS_00016233 is consistently elevated in septic AKI and non-AKI patients, and this peculiar lncRNA has a potential diagnosis value for septic AKI patients. In fact, inhibition of TCONS_00016233 ameliorated the renal cell apoptosis caused by LPS in HK-2 cells. Mechanistically, TCONS_00016233 acts as a ceRNA to prevent miR-22-3p-mediated downregulation of AIFM1 (Figure S5). Finally, overexpression of TCONS_00016233 can aggravate both LPS- and CLP-induced AKI via targeting the miR-22-3p/AIFM1 axis (Figures 10, S1, S2, and S3). Collectively, these findings demonstrate that TCONS_00016233 is a putative new marker of septic AKI, which may also modulate the progression of septic AKI.

Recent reports have examined the changes of lncRNAs in sepsis AKI and non-AKI patients.^{13,14} In our current study, we have precisely demonstrated that 203 lncRNAs are coregulated in sepsis patients. Among these, TCONS_00016233 was the most co-upregulated lncRNA in septic AKI (Figure 1; Table S1). The following series of evidences supported the notion that TCONS_00016233 might be an early, new marker of septic AKI. First, absolute quantitative PCR (qPCR) data were able to validate the finding of the lncRNA chip

assay and qRT-PCR in an expanded sample size (Figure 2A). Second, plasma TCONS_00016233 was elevated in sepsis non-AKI patients, but a higher cutoff threshold (9.5×10^5 copy number) provided a sensitivity of 71.9% and specificity of 89.6% for its detection in septic AKI (Figure 2B). Third, plasma TCONS_00016233 was not only highly correlated with serum creatinine (a traditional diagnostic indicator of renal injury) but also with TIMP-2 and IGFBP7, both US Food and Drug Administration (FDA)-approved diagnostic indicators for septic AKI and CRP, IL-1 β , and TNF- α (Figures 2C–2E and 2I–2K).^{18–21} Finally, the expression of urinary TCONS_00016233 was consistent and highly correlated with the levels of TCONS_00016233 in the plasma (Figures 2F and 2G). However, current data might be expanded and revalidated using a larger number of patients.

Several studies have reported that lncRNAs can be involved in the progression of septic AKI.^{22–26} For instance, the lncRNAs HOTAIR and TUG1 have shown a renoprotective role in septic AKI.^{23,24} Contrarily, other lncRNAs, like NEAT1 and PVT1, have an apparent opposing role in septic AKI.^{22,25} In the current study, we discovered that TCONS_00016233 is markedly induced by LPS via the TLR4/p38MAPK axis and located in the cytoplasm of HK-2 cells (Figure 3). Second, knockdown of TCONS_00016233 expression attenuated the LPS-induced renal cell apoptosis and the activation of caspase-3 (Figure 4). On the other hand, TCONS_00016233 overexpression was able to exacerbate these effects, accompanied by the increasing of IL-1 β and TNF- α (Figure 5). Moreover, overexpression of TCONS_00016233 exacerbated the LPS- and CLP-induced AKI, as demonstrated by the deterioration of renal function, aggravation of renal tubular damage, as well as increasing renal cell apoptosis (Figures 10 and S2). Altogether, the data suggest that TCONS_00016233 plays an injury-related role during septic AKI.

lncRNAs can possibly function as ceRNAs to regulate targeted mRNA expression.^{27–29} We predicted that miR-22-3p could directly bind to TCONS_00016233 (Figure 6A). To strengthen this hypothesis, a number of experiments were performed. First, dual-luciferase reporter assays demonstrated that miR-22-3p directly binds to TCONS_00016233 (Figure 6B). Second, RNA-FISH colocalization assays indicated that TCONS_00016233 interacts with miR-22-3p both *in vitro* and *in vivo* (Figures 6C and 6D). Finally, qRT-PCR data confirmed that LPS induces the expression of miR-22-3p, and this expression could be synergized by TCONS_00016233 overexpression or reversed by TCONS_00016233 silencing (Figures 6E

Figure 3. The TCONS_00016233 Was Induced by LPS

HK-2 cells were treated with 50 μ g/mL LPS, with or without TLR4 siRNA, p38MAPK agonist, or inhibitor. (A) RNA-FISH detection of intracellular localization of TCONS_00016233 in HK-2 cells. (B) qRT-PCR analysis of the expression levels of TCONS_00016233. (C) Immunoblot of phospho-p38 (p-p38)MAPK, p38MAPK, TLR4, and GAPDH. (D) Densitometric analysis of immunoblot bands. (E) qRT-PCR analysis of the expression levels of TCONS_00016233. (F) Immunoblot of p-p38MAPK, p38MAPK, and GAPDH. (G) Densitometric analysis of immunoblot bands. (H) qRT-PCR analysis of the expression levels of TCONS_00016233. (I) Immunoblot of p-p38MAPK, p38MAPK, TLR4, and GAPDH. (J) Densitometric analysis of immunoblot bands. (K) qRT-PCR analysis of the expression levels of TCONS_00016233. Data are expressed as mean \pm SD (n = 6). #p < 0.05, LPS at 12 h and 24 h groups versus control group. *p < 0.05, LPS/TLR4 siRNA, p38MAPK inhibitor/LPS, or LPS/TLR siRNA/p38MAPK agonist versus LPS/scramble group. Δ p > 0.05, LPS/TLR siRNA/p38MAPK agonist versus LPS/scramble group.

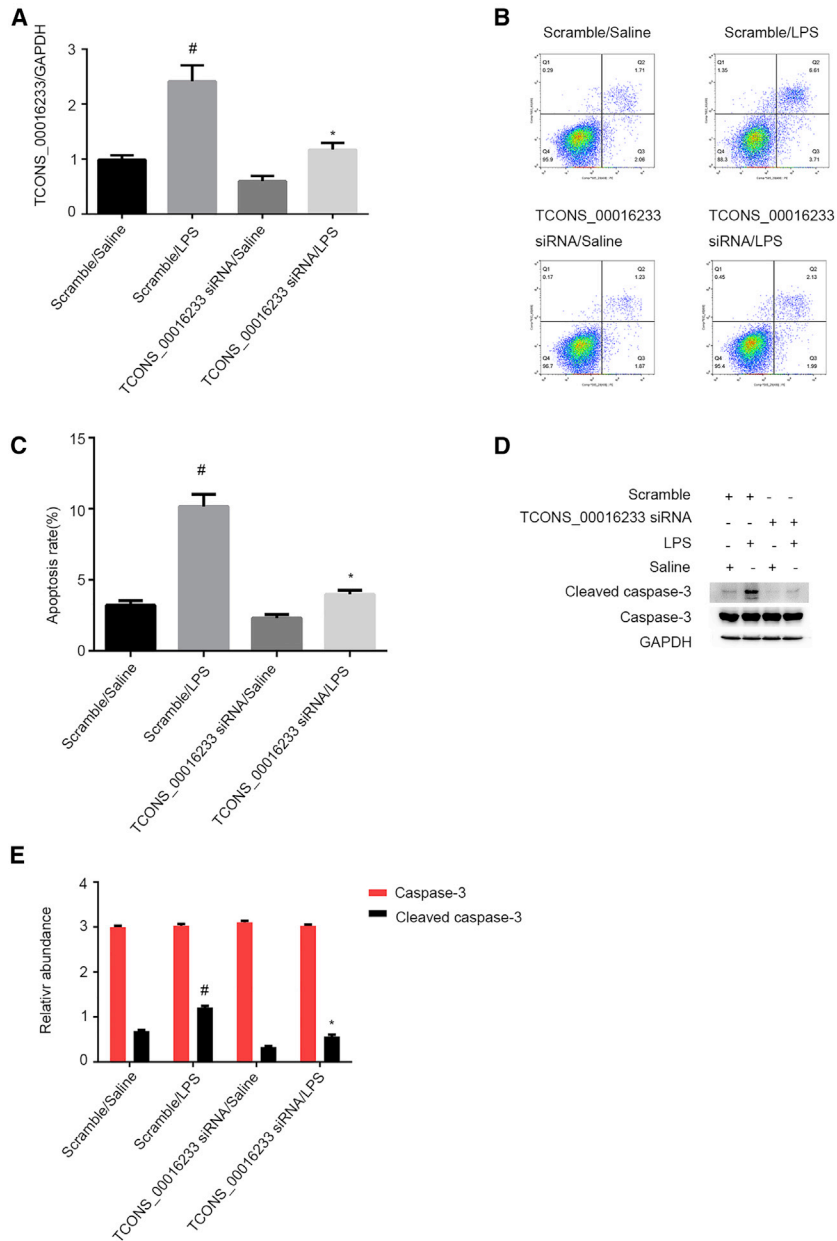


Figure 4. LPS-Induced HK-2 Cell Apoptosis Was Attenuated by siRNA of TCONS_00016233

HK-2 cells were transfected with 50 nM TCONS_00016233 siRNA or scramble and then treated with or without 50 μ g/mL LPS for 24 h. (A) qRT-PCR analysis of the expression levels of TCONS_00016233. (B and C) FCM analysis of HK-2 cell apoptosis. (D) Immunoblot analysis of cleaved caspase-3 and caspase-3. (E) Densitometric analysis of immunoblot bands. Data are expressed as mean \pm SD (n = 6). #p < 0.05, scramble with LPS or TCONS_00016233 siRNA group versus scramble with saline group; *p < 0.05, TCONS_00016233 siRNA with LPS group versus scramble with LPS group.

AIFM1, respectively (Figures 8C and 8D). Previous studies indicate that AIFM1 can mediate hepatoma cell apoptosis,¹⁵ which is consistent with our current findings, where AIFM1 knockdown significantly ameliorated LPS-induced renal cell apoptosis and caspase-3 activation *in vitro* (Figures 8E–8H). Here, a number of evidences supported that miR-22-3p/AIFM1 can mediate LPS-induced renal cell apoptosis. First, knockdown of TCONS_00016233 expression attenuates LPS-induced renal cell apoptosis, and this effect is diminished by the inhibition of miR-22-3p to increase AIFM1 (Figure 9). In addition, overexpression of TCONS_00016233 aggravates LPS- and CLP-induced AKI by targeting miR-22-3p/AIFM1 axis and upregulation of IL-1 β and TNF- α (Figures S1 and S3). Taken together, these data suggest that TCONS_00016233 promotes LPS-induced renal cell apoptosis by regulating the miR-22-3p/AIFM1 axis.

In conclusion, here, we found that plasma TCONS_00016233 has high sensitivity and specificity for the diagnosis of septic AKI. TCONS_00016233 mediates LPS-induced renal cell apoptosis *in vitro*. For this, it directly binds to miR-22-3p to increase AIFM1 expression, leading to renal cell apoptosis. Overexpression of TCONS_00016233 aggravates both LPS- and CLP-induced AKI *in vivo* via targeting the miR-22-3p/AIFM1 axis. Collectively, our data suggest

that TCONS_00016233 has the potential to act as a reliable biomarker for septic AKI and may also serve as a novel therapeutic target for septic AKI.

MATERIALS AND METHODS

Antibodies and Reagents

AIFM1 (Cat. No. 17984-1-AP) and glyceraldehyde 3-phosphate dehydrogenase (GAPDH) (Cat. No. 10494-1-AP) were purchased from Proteintech North America (Rosemont, IL, USA). Caspase-3 (Cat. No. 9662S) and cleaved caspase-3 (Cat. No. 9661) were obtained from Cell Signaling Technology (Danvers, MA, USA). Luciferase

and 6F). Collectively, these data strongly suggest that miR-22-3p is a direct target of TCONS_00016233.

So far, only one study has demonstrated that miR-22-3p has an anti-apoptotic role.¹⁶ Still, a putative role in LPS-induced renal cell apoptosis was still unknown. In the present study, FCM analysis and immunoblot of cleaved caspase-3 demonstrated that miR-22-3p mimics notably suppressed the LPS-induced renal cell apoptosis *in vitro* (Figure 7). We further suggested that miR-22-3p could directly bind to AIFM1 (Figures 8A and 8B). qRT-PCR and immunoblot results further indicated that, in fact, miR-22-3p mimics suppress mRNA levels and protein expression of

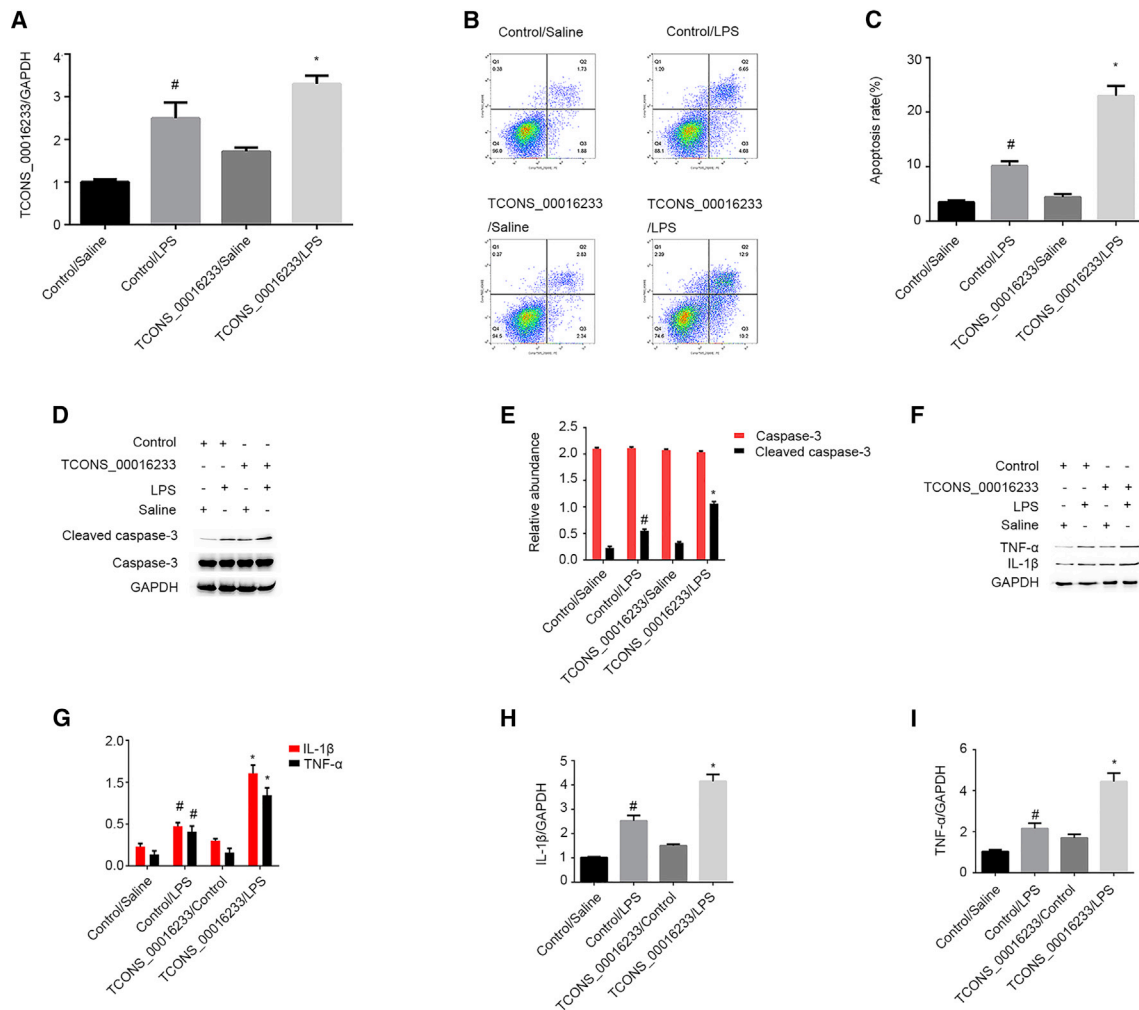


Figure 5. LPS-Induced HK-2 Cell Apoptosis Was Enhanced by Overexpression of TCONS_00016233

HK-2 cells were transfected with TCONS_00016233 plasmid or control and then treated with or without 50 μg/mL LPS for 24 h. (A) qRT-PCR analysis of the expression levels of TCONS_00016233. (B and C) FCM analysis of HK-2 cell apoptosis. (D) Immunoblot analysis of cleaved caspase-3 and caspase-3. (E) Densitometric analysis of immunoblot bands. (F and G) qRT-PCR analysis of the expression levels of IL-1β and TNF-α. (H) Immunoblot analysis of the expression levels of IL-1β and TNF-α. (I) Densitometric analysis of immunoblot bands. Data are expressed as mean ± SD (n = 6). #p < 0.05, scramble with LPS or TCONS_00016233 group versus scramble with saline group; *p < 0.05, TCONS_00016233 with LPS group versus scramble with LPS group.

assay kit was purchased from BioVision (Milpitas, CA, USA). The fluorescein isothiocyanate (FITC) Annexin V Apoptosis Detection Kit I (Cat. No. 556547) was obtained from BD Pharmingen (Franklin, NJ, USA). p38 MAPK inhibitor (Cat. #HY-10256/CS-0140) and p38MAPK agonist (Cat. #HY-N0674A/CS-6061) were purchased from MedChemExpress USA (Deer Park, NJ, USA). Antibody TNF-α (17590-1-AP), IL-1β (16806-1-AP), and TLR4 (19811-1-AP) were from Proteintech North America (Rosemont, IL, USA). p38MAPK (ab31828) was from Abcam (Cambridge, MA, USA). Phospho-p38MAPK (Cat. #4511s) was from Cell Signaling Technology (Danvers, MA, USA). An ELISA kit for IL-1β (ab100562), TNF-α (ab181421), TIMP-2 (Cat. No. DTM200), and IGFBP7 (Cat. No. DY1334-05) was purchased from R&D Systems (Minneapolis, MN, USA).

Cell Culture and Treatments

HK-2 cells were cultured in DMEM (Sigma-Aldrich), supplemented with 10% fetal bovine serum (FBS) and 1% penicillin-streptomycin (10,000 U/mL and 10,000 g/mL, respectively), and incubated at 37°C under a humidified atmosphere of 5% CO₂. HK-2 cells were treated with saline or LPS (50 μg/mL) for 24 h. For gene-silencing procedures, cells were transfected with miR-22-3p antagonist (100 nM), miR-22-3p mimic (100 nM), TCONS_00016233 siRNA (100 nM), AIFM1 siRNA (100 nM), or negative control (Ruibo, Guangzhou, China) using Lipofectamine 2000 (Life Technologies, Carlsbad, CA, USA).

Human Samples

The research protocol was approved by the Second Xiangya Hospital Review Board, The People's Republic of China Hospital. Written,

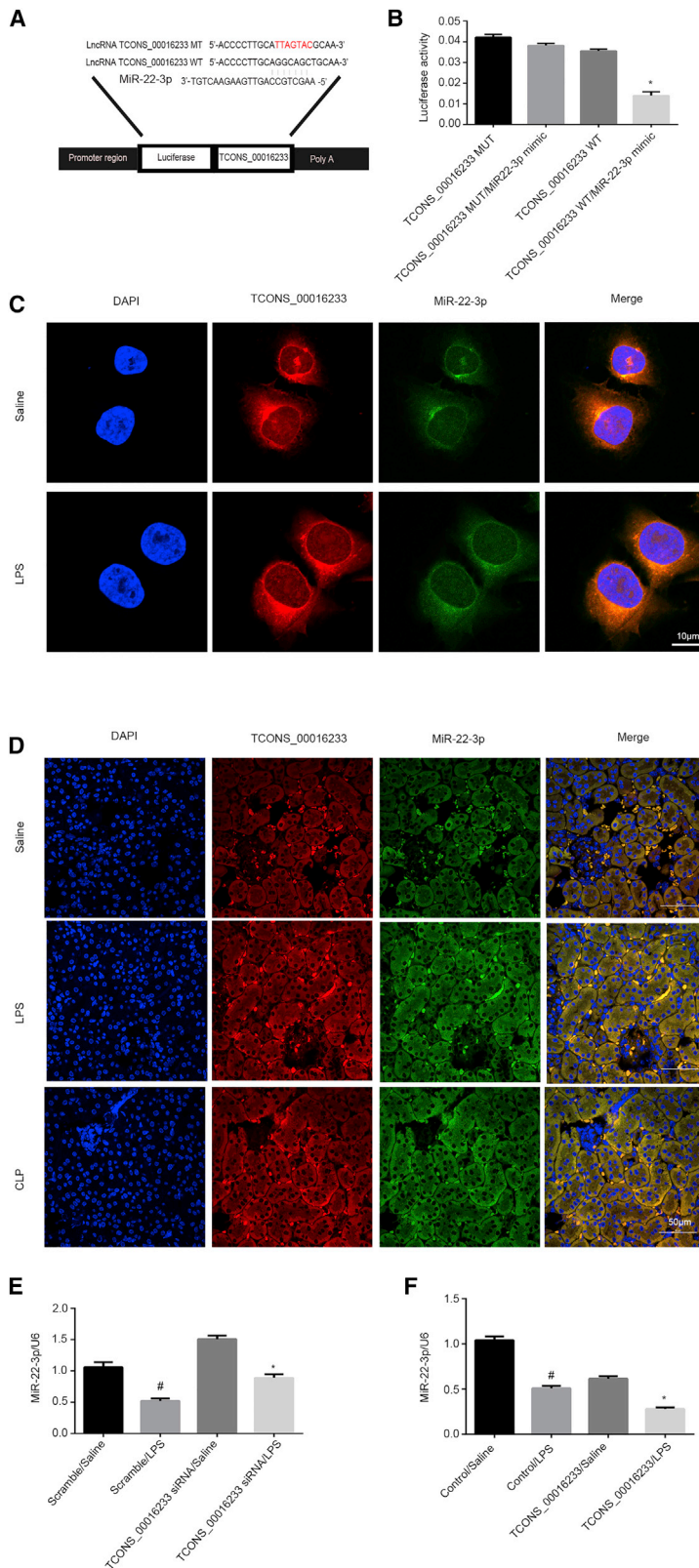


Figure 6. TCONS_00016233 Directly Bound to miR-22-3p

(A) Sequence alignment analysis showed that TCONS_00016233 contained the complementary chain with miR-22-3p. (B) Detection of luciferase activities after cotransfection with TCONS_00016233-WT or TCONS_00016233-MUT and miR-22-3p or scramble. (C and D) Intracellular colocalization of TCONS_00016233 and miR-22-3p in HK-2 cells treated with or without LPS treatment and kidney samples from a LPS- or CLP-induced AKI model. (E and F) qRT-PCR analysis of TCONS_00016233 expression. # $p < 0.05$, scramble with LPS group versus scramble with saline group; * $p < 0.05$, TCONS_00016233 siRNA or TCONS_00016233 with LPS group versus scramble with LPS group.

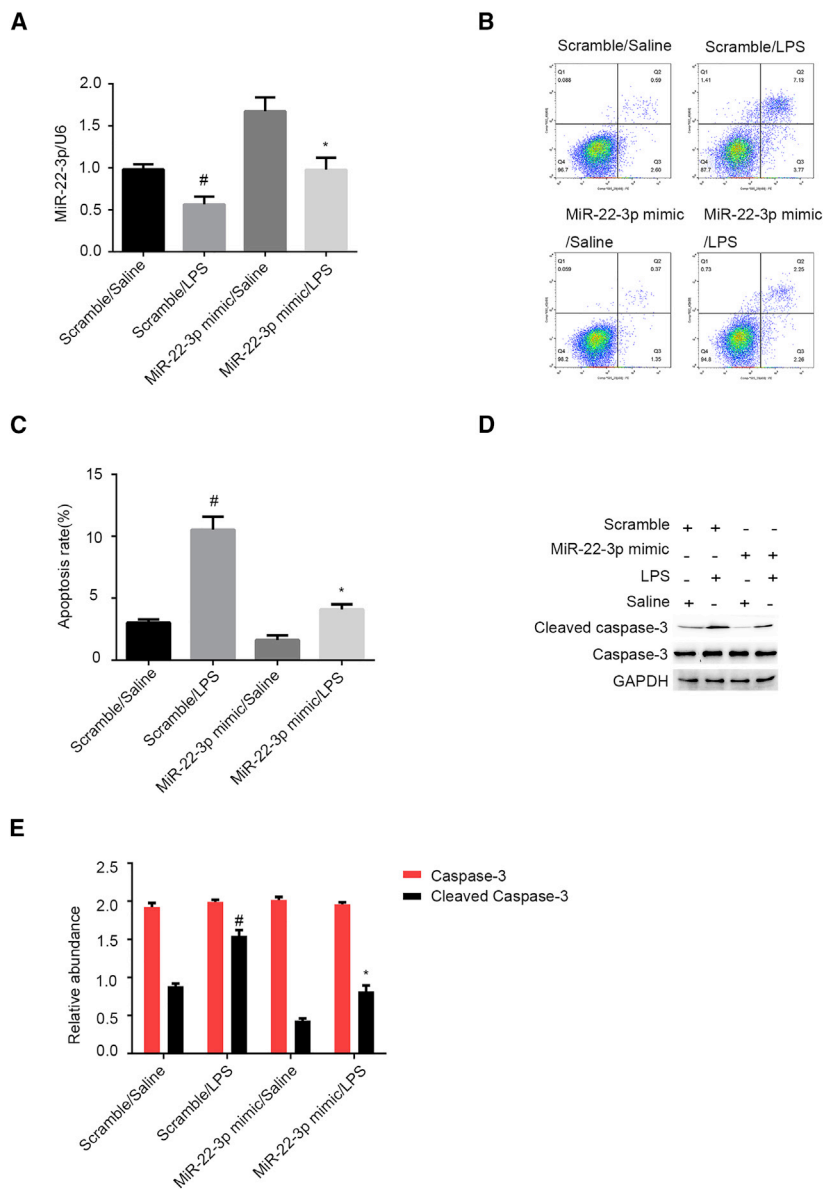


Figure 7. LPS-Induced HK-2 Cell Apoptosis Was Attenuated by miR-22-3p Mimics

HK-2 cells were transfected with 100 nM miR-22-3p mimics or scramble and then treated with or without 50 μg/mL LPS for 24 h. (A) qRT-PCR analysis of miR-22-3p expression. (B and C) FCM analysis of HK-2 cell apoptosis. (D) Immunoblot analysis of cleaved caspase-3 and caspase-3. (E) Densitometric analysis of immunoblot bands. Data are expressed as mean ± SD (n = 6). #p < 0.05, scramble with LPS group versus scramble with saline group; *p < 0.05, miR-22-3p mimics with LPS versus scramble with LPS group.

(WT-Luc-TCONS_00016233) and AIFM1-3' UTR (WT-Luc-AIFM1) contained, respectively, responsive elements of TCONS_00016233 and AIFM1 interaction with miR-22-3p. The mutated plasmids for TCONS_00016233 (MUT-Luc-TCONS_00016233) and AIFM1 (MUT-Luc-AIFM1) lacked these responsive elements. pGMLR-TK luciferase vector expressing Renilla luciferase (RLuc) was used as an internal control. All plasmids were engineered by RuQi Biotechnology (Guanzhou, Guangdong, China).

To perform the assay, the pGMLR-TK plasmid was co-transfected with WT-Luc-TCONS_00016233 or MUT-Luc-TCONS_00016233, with or without miR-22-3p mimics, in HK-2 cells. After 48 h of transfection, the luciferase reporter assay was carried out as previously described.^{29,32,33} A SpectraMax M5 (Molecular Devices, Sunnyvale, CA, USA) was used to examine the gene reporter activity and normalized by the RLuc signal.

Animal Models

C57BL/6J mice (male, aged 10–12 weeks) were pre-injected with TCONS_00016233 or control-expressing vectors via tail vein (25 μg of DNA per injection) and then injected intraperitoneally with lipopolysaccharides (LPS) at a dose of 10 mg/kg. Alternatively, animals were subjected to CLP to induce AKI, according to that previously described.³⁴ The saline injection or sham operation was considered as a control group. 24 h after LPS treatment or 18 h following CLP treatment, renal tissues were collected for renal function and morphology analyses. Animal experiments were performed in strict accordance with the recommendations of the Institutional Committee for the Care and Use of Laboratory Animals of Second Xiangya Hospital (China). All animals were allowed free access to food and water at any time and housed on a 12-h light/dark cycle.

informed consent was gotten from all individual participants. Sepsis was defined according to consensus guidelines.³⁰ AKI was defined according to the KDIGO criteria.³¹ Human blood and urine samples from healthy volunteers (n = 30), sepsis patients with AKI (n = 96), and sepsis patients without AKI (n = 96) were collected accordingly. Blood samples were centrifuged to obtain plasma or serum and then stored at -80°C.

Luciferase Reporter Assays

The microRNA (miRNA) activity was evaluated via the insertion of miRNA target sites at the 3' end of the firefly luciferase gene (luc2) using the pmirGLO dual-luciferase miRNA target expression vector (Promega, Madison, WI, USA). The luciferase vectors for TCONS_00016233

Renal Function, Morphological Studies, and Apoptosis

The levels of BUN and creatinine were evaluated as previously described.³⁵ Experimental procedures followed the manufacturer's protocol (Nanjing Jiancheng Bioengineering Institute, Jiangsu, China). To

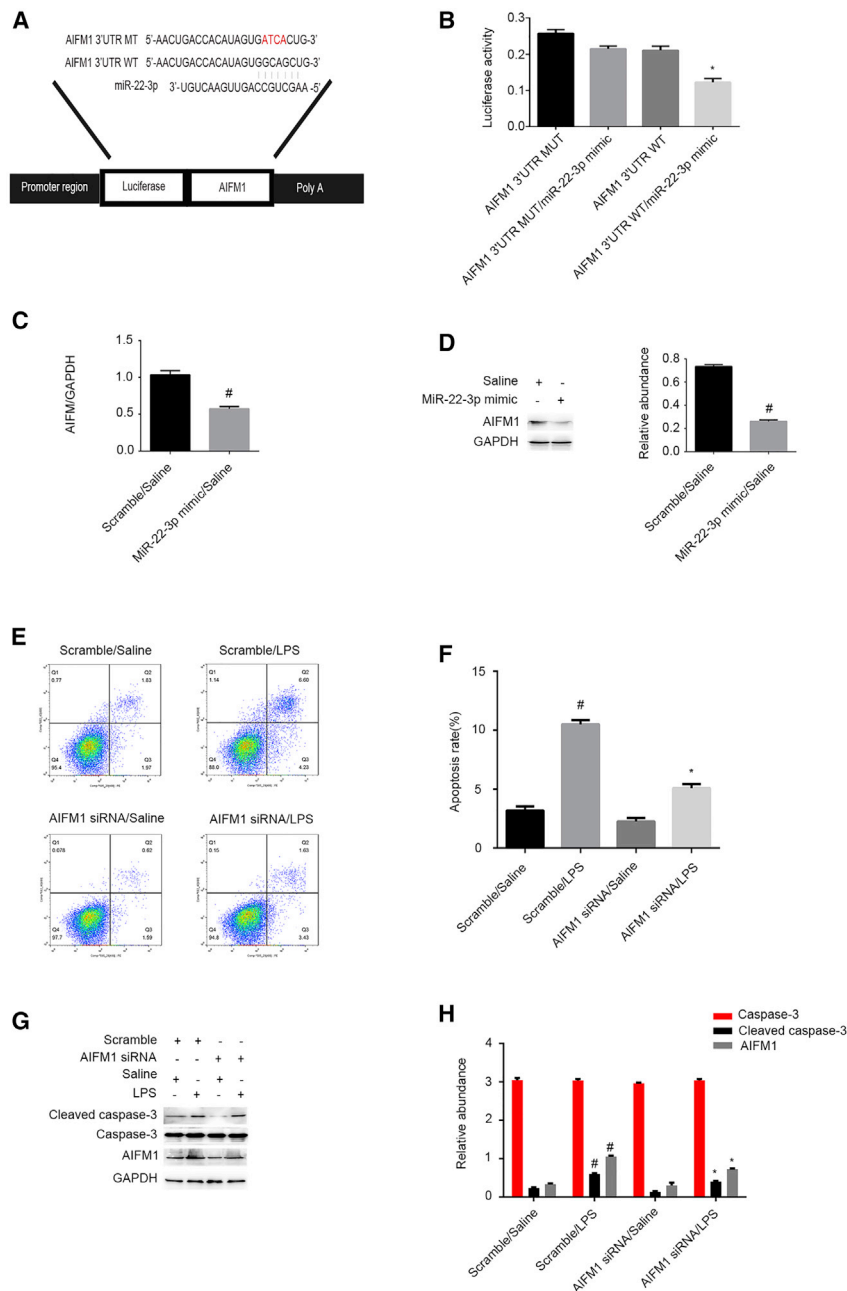


Figure 8. AIFM1 Was Identified As a Target Gene of miR-22-3p and Mediates the Renal Cell Apoptosis

HK-2 cells were transfected with 100 nM miR-22-3p mimics or siRNA AIFM1 or scramble and then treated with or without 50 μ g/mL LPS for 24 h. (A) Putative miR-22-3p complementary binding sites in the 3' UTR of human AIFM1 mRNA. (B) Measurement of luciferase activities after co-transfection with the 3' UTR luciferase reporter vector of human WT- or MUT-AIFM1 and miR-22-3p or miR-negative control (NC). (C and D) The qRT-PCR and western blot analysis of AIFM1 and GAPDH. (E and F) FCM analysis of HK-2 cell apoptosis. (G) Immunoblot analysis of cleaved caspase-3, caspase-3, and AIFM1. (H) Densitometric analysis of immunoblot bands. Data are expressed as mean \pm SD (n = 6). #p < 0.05, scramble with LPS group versus scramble with saline group; *p < 0.05, AIFM1 siRNA with LPS versus scramble with LPS group or AIFM1 3' UTR WT plus miR-22-3p mimics versus other groups.

tech, Shanghai, China), which contained 30,586 lncRNAs and 26,109 coding transcripts. Scanning was performed with an AxonGenePix 4000B microarray scanner. GenePix Pro v6.0 was used to read the raw image intensity.

Relative and Absolute qPCR

Trizol Reagent (Invitrogen, Carlsbad, CA, USA) was applied to extract total RNA from plasma, HK-2 cells, and kidney of C57BL/6J mice, in accordance with the manufacturer's procedure. Total RNA (40 ng) was reverse transcribed using Moloney Murine Leukemia Virus (M-MLV) Reverse Transcriptase (Invitrogen). Real-time qPCR was carried out to detect the expression levels of miRNA, mRNA, and lncRNA using Bio-Rad (Hercules, CA, USA) iQ SYBR Green Supermix with Opticon (MJ Research, Waltham, MA, USA), according to the manufacturer's protocol. The sequences of TCONS_00016233 and miR-22-3p were retrieved from the GenBank database (GenBank: NC_000009.12 and 407004, respectively). The primers used were as follows: TCONS_00016233: 5'-CAGAGCAAGGGAACAGTAAGTGTGT-3' (forward) and 5'-GGAGGTCACCTCCGATC CA-3' (reverse); miR-22-3p: 5'-GCGAAGCTGCCAGTTGAAG-3' (forward) and 5'-AGTGCAGGGTCCGAGGTATT-3' (reverse); and GAPDH: 5'-GGTCTCTCTGACTTCACA-3' (forward) and 5'-GTGAGGGTCTCTCTTCTTCT-3' (reverse). U6 primers were described previously.⁴⁰ For the absolute quantitative real-time PCR, the standard control sequence of TCONS_00016233(5'-CAGA GCAAGGGAACAGTAAGTGTGTCTTGGAGGCGCTCGCCATG CACTCACACGCCATCTGTGGATTTCGGAAGTGACCTCC-3') was used, which was cloned into the pUC57 plasmid. The sequence of the probe of TCONS_00016233 was used as follows: 5'-TC

assess the degree of tissue damage, H&E staining was performed accordingly.³⁶⁻³⁹ TUNEL staining was also utilized to detect renal cell apoptosis and quantified by counting the percentage of positive staining cells, according to the previous study.³⁷ An Olympus microscope equipped with UV epi-illumination was used to analyze the stained samples. FCM procedures were carried out according to the manufacturer's protocol.

lncRNA Microarray

lncRNA and mRNA transcriptome analyses were carried out using the Arraystar Human lncRNA V3.0 microarray (KangChen Bio-

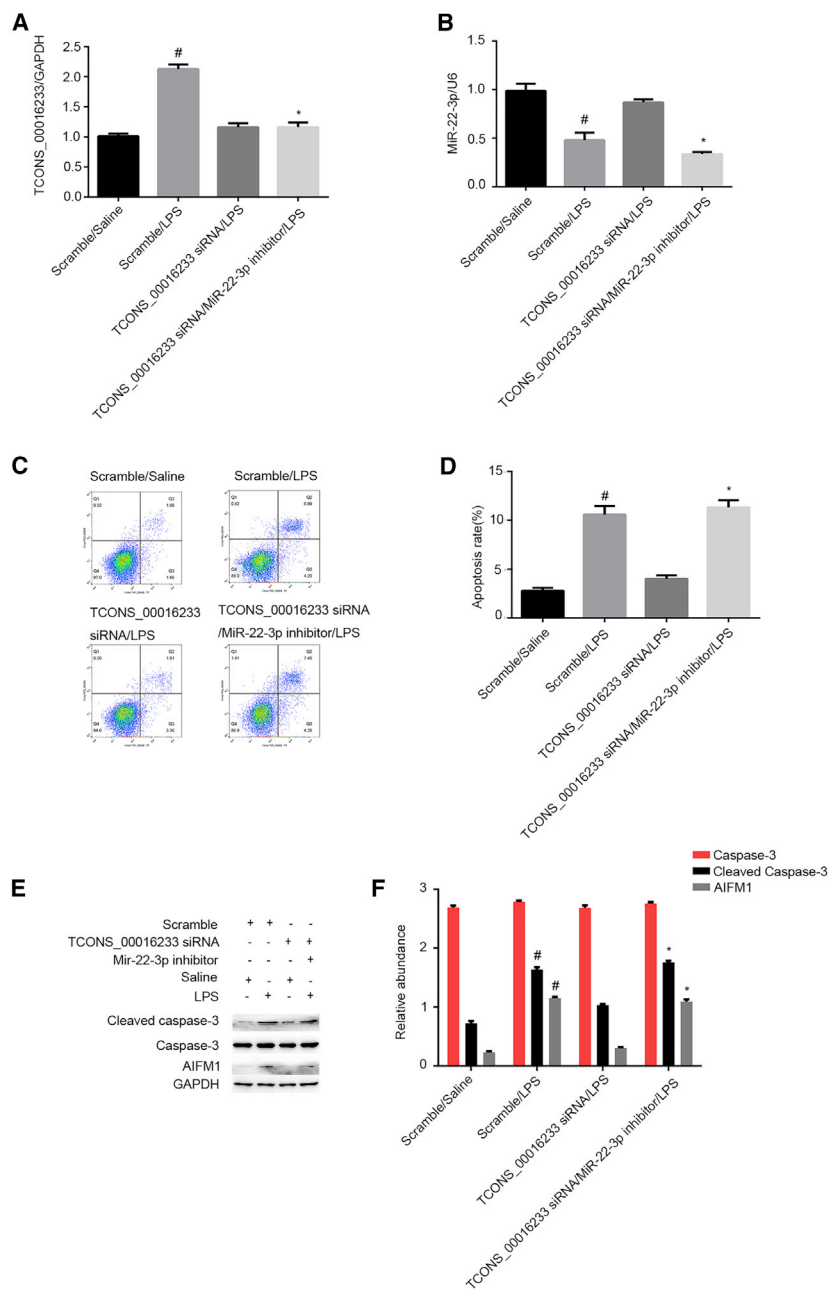


Figure 9. Inhibition of TCONS_00016233 Attenuated the LPS-Induced HK-2 Cell Apoptosis, Which Was Reversed by the miR-22-3p Inhibitor

HK-2 cells were cotransfected with TCONS_00016233 (100 nM) and anti-miR-22-3p or scramble and then treated with LPS for 24 h. (A and B) qRT-PCR analysis of the expression levels of TCONS_00016233 and miR-22-3p. (C and D) FCM analysis of HK-2 cell apoptosis. (E) Immunoblot analysis of cleaved caspase-3 and caspase-3. (F) Densitometric analysis of immunoblot bands. Data are expressed as mean \pm SD (n = 6). #p < 0.05, scramble or TCONS_00016233 siRNA with LPS group versus scramble group; *p < 0.05, TCONS_00016233 siRNA plus anti-miR-22-3p with LPS group versus TCONS_00016233 siRNA with LPS group.

GAPDH, followed by incubation with secondary antibody and detection reagents. GAPDH was used as an internal loading control.

FISH

The fluorescence probes of TCONS_00016233 (5'-TCGCCATGCACTCACAGCCAT-3') and miR-22-3p (5'-ACAGUUCUUAACUGGCAGC UU-3') were synthesized by Ruibo (Guangzhou, China). To detect in HK-2 cells, nuclei was stained with 4',6-diamidino-2-phenylindole (DAPI), U6 (nucleus positive), and 18S rRNA (cytoplasmic positive), and TCONS_00016233 was labeled by CY3. Briefly, the slides of HK-2 cells and mice kidney were hybridized overnight with respective probes and subsequently stained with DAPI. A laser-scanning confocal microscope was used for fluorescence imaging analysis.

Statistical Analyses

Two-tailed Student's t tests were used for comparing the difference between two groups. One-way ANOVA was performed for multiple group comparison. The χ^2 test was used to compare the categorical variables. Quantitative data were expressed as mean \pm standard deviation (SD). The Spearman rank correlation coefficient

was used to assess the correlations between variables. To evaluate the diagnostic value of lncRNAs, ROC curves were produced, and the AUCs were counted. All statistical analyses were performed with the SPSS package (SPSS) and GraphPad Prism software (GraphPad Prism Software). p < 0.05 was considered statistically significant.

SUPPLEMENTAL INFORMATION

Supplemental Information can be found online at <https://doi.org/10.1016/j.omtn.2019.12.037>.

GCCATGCACTCACAGCCAT-3'. Δ Ct values were used to perform the relative quantification. The absolute quantification was carried out according to a standard curve.

Immunoblot Analysis

Equal amounts of proteins were resolved by SDS-PAGE and then transferred to a nitrocellulose membrane (Amersham, Buckinghamshire, UK).^{34,35,40-42} Respective blots were subsequently probed with primary antibodies against AIFM1, caspase-3, cleaved caspase-3, and

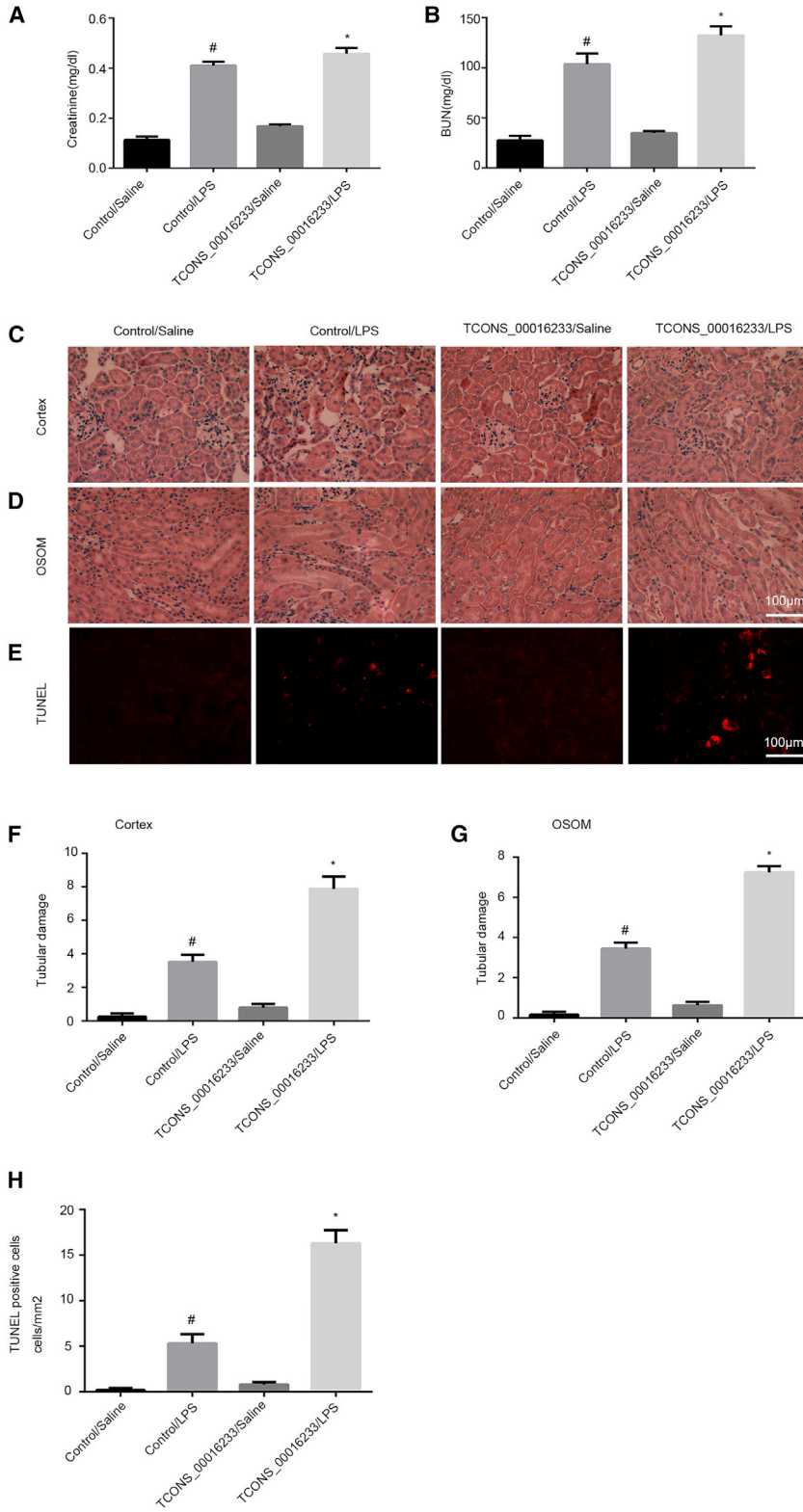


Figure 10. LPS-Induced AKI Was Aggravated by the Overexpression of TCONS_00016233 in Male C57BL/6 Mice

C57BL/6J mice were pretreated with the TCONS_00016233 plasmid via tail vein for 12 h and then injected with 10 mg/kg LPS for 24 h saline as control. (A and B) Blood serum was obtained for detection of nitrogen (BUN) (A) and creatinine (B) concentration. (C–E) The sections of kidney (cortex in C and OSOM in D) were stained with hematoxylin and eosin (H&E) and TUNEL (E). (F and G) Tubular damage scores of kidney cortex (F) and OSOM (G). (H) Counting of TUNEL-positive cells. Data are expressed as mean ± SD (n = 6). #p < 0.05, control with LPS group versus saline group; *p < 0.05, TCONS_00016233 plasmid with LPS group versus control with LPS group. Original magnification, ×200.

AUTHOR CONTRIBUTIONS

D.Z. designed this study. P.Z. and L.Y. performed the experiments. S.Q., J.D., Y.L., X.L., K.A., H.L., S.Q., and Y.W. collected the data. Statistical analysis and reagent purchasing were carried out by X.X. and Z.D. D.Z. wrote the manuscript.

CONFLICTS OF INTEREST

The authors declare no competing interests.

ACKNOWLEDGMENTS

The National Natural Science Foundation of China (81870475, 81570646, and 81770951), Hunan Province Natural Science Foundation (2018JJ2568), and Youth Foundation of Hu'nan Scientific Committee (2017JJ1035) supported this study, as well as the Changsha Science and Technology Bureau Project (kq1901115).

REFERENCES

- Hoste, E.A., Bagshaw, S.M., Bellomo, R., Cely, C.M., Colman, R., Cruz, D.N., Edipidis, K., Forni, L.G., Gomersall, C.D., Govil, D., et al. (2015). Epidemiology of acute kidney injury in critically ill patients: the multinational AKI-EPI study. *Intensive Care Med.* *41*, 1411–1423.
- Rewa, O., and Bagshaw, S.M. (2014). Acute kidney injury-epidemiology, outcomes and economics. *Nat. Rev. Nephrol.* *10*, 193–207.
- Chertow, G.M., Burdick, E., Honour, M., Bonventre, J.V., and Bates, D.W. (2005). Acute kidney injury, mortality, length of stay, and costs in hospitalized patients. *J. Am. Soc. Nephrol.* *16*, 3365–3370.
- Wang, K., Xie, S., Xiao, K., Yan, P., He, W., and Xie, L. (2018). Biomarkers of Sepsis-Induced Acute Kidney Injury. *BioMed Res. Int.* *2018*, 6937947.
- Su, L., Xie, L., and Liu, D. (2015). Urine sTREM-1 may be a valuable biomarker in diagnosis and prognosis of sepsis-associated acute kidney injury. *Crit. Care* *19*, 281.
- Bagshaw, S.M., Bennett, M., Haase, M., Haase-Fielitz, A., Egi, M., Morimatsu, H., D'Amico, G., Goldsmith, D., Devarajan, P., and Bellomo, R. (2010). Plasma and urine neutrophil gelatinase-associated lipocalin in septic versus non-septic acute kidney injury in critical illness. *Intensive Care Med.* *36*, 452–461.
- Kashani, K., Al-Khafaji, A., Ardiles, T., Artigas, A., Bagshaw, S.M., Bell, M., Bihorac, A., Birkhahn, R., Cely, C.M., Chawla, L.S., et al. (2013). Discovery and validation of cell cycle arrest biomarkers in human acute kidney injury. *Crit. Care* *17*, R25.
- Han, W.K., Bailly, V., Abichandani, R., Thadhani, R., and Bonventre, J.V. (2002). Kidney Injury Molecule-1 (KIM-1): a novel biomarker for human renal proximal tubule injury. *Kidney Int.* *62*, 237–244.
- Valette, X., Savary, B., Nowoczyn, M., Daubin, C., Pottier, V., Terzi, N., Seguin, A., Fradin, S., Charbonneau, P., Hanouz, J.L., and du Cheyron, D. (2013). Accuracy of plasma neutrophil gelatinase-associated lipocalin in the early diagnosis of contrast-induced acute kidney injury in critical illness. *Intensive Care Med.* *39*, 857–865.
- Li, Q., Shao, Y., Zhang, X., Zheng, T., Miao, M., Qin, L., Wang, B., Ye, G., Xiao, B., and Guo, J. (2015). Plasma long noncoding RNA protected by exosomes as a potential stable biomarker for gastric cancer. *Tumour Biol.* *36*, 2007–2012.
- Huang, X., Yuan, T., Tschannen, M., Sun, Z., Jacob, H., Du, M., Liang, M., Dittmar, R.L., Liu, Y., Liang, M., et al. (2013). Characterization of human plasma-derived exosomal RNAs by deep sequencing. *BMC Genomics* *14*, 319.
- Meng, Q., Wang, K., Brunetti, T., Xia, Y., Jiao, C., Dai, R., Fitzgerald, D., Thomas, A., Jay, L., Eckart, H., et al. (2018). The *DGCR5* long noncoding RNA may regulate expression of several schizophrenia-related genes. *Sci. Transl. Med.* *10*, eaat6912.
- Dai, Y., Liang, Z., Li, Y., Li, C., and Chen, L. (2017). Circulating Long Noncoding RNAs as Potential Biomarkers of Sepsis: A Preliminary Study. *Genet. Test. Mol. Biomarkers* *21*, 649–657.
- Lorenzen, J.M., Schauerte, C., Kielstein, J.T., Hübner, A., Martino, F., Fiedler, J., Gupta, S.K., Faulhaber-Walter, R., Kumarswamy, R., Hafer, C., et al. (2015). Circulating long noncoding RNAs are a predictor of mortality in critically ill patients with acute kidney injury. *Clin. Chem.* *61*, 191–201.
- Havasi, A., and Borkan, S.C. (2011). Apoptosis and acute kidney injury. *Kidney Int.* *80*, 29–40.
- Lv, K.T., Liu, Z., Feng, J., Zhao, W., Hao, T., Ding, W.Y., Chu, J.P., and Gao, L.J. (2018). MiR-22-3p Regulates Cell Proliferation and Inhibits Cell Apoptosis through Targeting the eIF4EBP3 Gene in Human Cervical Squamous Carcinoma Cells. *Int. J. Med. Sci.* *15*, 142–152.
- Liu, D., Liu, M., Wang, W., Pang, L., Wang, Z., Yuan, C., and Liu, K. (2018). Overexpression of apoptosis-inducing factor mitochondrion-associated 1 (AIFM1) induces apoptosis by promoting the transcription of caspase3 and DRAM in hepatoma cells. *Biochem. Biophys. Res. Commun.* *498*, 453–457.
- Guzzi, L.M., Bergler, T., Binnall, B., Engelman, D.T., Forni, L., Germain, M.J., Gluck, E., Göcze, I., Joannidis, M., Koyner, J.L., et al. (2019). Clinical use of [TIMP-2]•[IGFBP7] biomarker testing to assess risk of acute kidney injury in critical care: guidance from an expert panel. *Crit. Care* *23*, 225.
- Xie, Y., Ankawi, G., Yang, B., Garzotto, F., Passannante, A., Breglia, A., Digvijay, K., Ferrari, F., Brendolan, A., Raffaele, B., et al. (2019). Tissue inhibitor metalloproteinase-2 (TIMP-2) • IGF-binding protein-7 (IGFBP7) levels are associated with adverse outcomes in patients in the intensive care unit with acute kidney injury. *Kidney Int.* *95*, 1486–1493.
- Adler, C., Heller, T., Schregel, F., Hagmann, H., Hellmich, M., Adler, J., and Reuter, H. (2018). TIMP-2/IGFBP7 predicts acute kidney injury in out-of-hospital cardiac arrest survivors. *Crit. Care* *22*, 126.
- Koyner, J.L., Shaw, A.D., Chawla, L.S., Hoste, E.A., Bihorac, A., Kashani, K., Haase, M., Shi, J., and Kellum, J.A.; Sapphire Investigators (2015). Tissue Inhibitor Metalloproteinase-2 (TIMP-2)•IGF-Binding Protein-7 (IGFBP7) Levels Are Associated with Adverse Long-Term Outcomes in Patients with AKI. *J. Am. Soc. Nephrol.* *26*, 1747–1754.
- Jiang, X., Li, D., Shen, W., Shen, X., and Liu, Y. (2019). LncRNA NEAT1 promotes hypoxia-induced renal tubular epithelial apoptosis through downregulating miR-27a-3p. *J. Cell. Biochem.* *120*, 16273–16282.
- Jiang, Z.J., Zhang, M.Y., Fan, Z.W., Sun, W.L., and Tang, Y. (2019). Influence of lncRNA HOTAIR on acute kidney injury in sepsis rats through regulating miR-34a/Bcl-2 pathway. *Eur. Rev. Med. Pharmacol. Sci.* *23*, 3512–3519.
- Liu, X., Hong, C., Wu, S., Song, S., Yang, Z., Cao, L., Song, T., and Yang, Y. (2019). Downregulation of lncRNA TUG1 contributes to the development of sepsis-associated acute kidney injury via regulating miR-142-3p/sirtuin 1 axis and modulating NF-κB pathway. *J. Cell. Biochem.* *120*, 11331–11341.
- Chen, Y., Qiu, J., Chen, B., Lin, Y., Chen, Y., Xie, G., Qiu, J., Tong, H., and Jiang, D. (2018). Long non-coding RNA NEAT1 plays an important role in sepsis-induced acute kidney injury by targeting miR-204 and modulating the NF-κB pathway. *Int. Immunopharmacol.* *59*, 252–260.
- Huang, W., Lan, X., Li, X., Wang, D., Sun, Y., Wang, Q., Gao, H., and Yu, K. (2017). Long non-coding RNA PVT1 promote LPS-induced septic acute kidney injury by regulating TNFα and JNK/NF-κB pathways in HK-2 cells. *Int. Immunopharmacol.* *47*, 134–140.
- Yi, H., Peng, R., Zhang, L.Y., Sun, Y., Peng, H.M., Liu, H.D., Yu, L.J., Li, A.L., Zhang, Y.J., Jiang, W.H., and Zhang, Z. (2017). LincRNA-Gm4419 knockdown ameliorates NF-κB/NLRP3 inflammasome-mediated inflammation in diabetic nephropathy. *Cell Death Dis.* *8*, e2583.
- Li, A., Peng, R., Sun, Y., Liu, H., Peng, H., and Zhang, Z. (2018). LincRNA 1700020114Rik alleviates cell proliferation and fibrosis in diabetic nephropathy via miR-34a-5p/Sirt1/HIF-1α signaling. *Cell Death Dis.* *9*, 461.
- Li, P., Zhang, X., Wang, L., Du, L., Yang, Y., Liu, T., Li, C., and Wang, C. (2017). lncRNA HOTAIR Contributes to 5FU Resistance through Suppressing miR-218 and Activating NF-κB/TS Signaling in Colorectal Cancer. *Mol. Ther. Nucleic Acids* *8*, 356–369.
- Rhodes, A., Evans, L.E., Alhazzani, W., Levy, M.M., Antonelli, M., Ferrer, R., Kumar, A., Sevransky, J.E., Sprung, C.L., Nunnally, M.E., et al. (2017). Surviving Sepsis Campaign: International Guidelines for Management of Sepsis and Septic Shock: 2016. *Crit. Care Med.* *45*, 486–552.

31. Drüeke, T.B., and Parfrey, P.S. (2012). Summary of the KDIGO guideline on anemia and comment: reading between the (guide)line(s). *Kidney Int.* 82, 952–960.
32. Sun, C.C., Zhang, L., Li, G., Li, S.J., Chen, Z.L., Fu, Y.F., Gong, F.Y., Bai, T., Zhang, D.Y., Wu, Q.M., and Li, D.J. (2017). The lncRNA PDIA3P Interacts with miR-185-5p to Modulate Oral Squamous Cell Carcinoma Progression by Targeting Cyclin D2. *Mol. Ther. Nucleic Acids* 9, 100–110.
33. Liu, X., Zheng, J., Xue, Y., Qu, C., Chen, J., Wang, Z., Li, Z., Zhang, L., and Liu, Y. (2018). Inhibition of TDP43-Mediated SNHG12-miR-195-SOX5 Feedback Loop Impeded Malignant Biological Behaviors of Glioma Cells. *Mol. Ther. Nucleic Acids* 10, 142–158.
34. Xu, X., Wang, J., Yang, R., Dong, Z., and Zhang, D. (2017). Genetic or pharmacologic inhibition of EGFR ameliorates sepsis-induced AKI. *Oncotarget* 8, 91577–91592.
35. Xu, L., Li, X., Zhang, F., Wu, L., Dong, Z., and Zhang, D. (2019). EGFR drives the progression of AKI to CKD through HIPK2 overexpression. *Theranostics* 9, 2712–2726.
36. Xu, X., Pan, J., Li, H., Li, X., Fang, F., Wu, D., Zhou, Y., Zheng, P., Xiong, L., and Zhang, D. (2019). Atg7 mediates renal tubular cell apoptosis in vancomycin nephrotoxicity through activation of PKC- δ . *FASEB J.* 33, 4513–4524.
37. Zhang, D., Pan, J., Xiang, X., Liu, Y., Dong, G., Livingston, M.J., Chen, J.K., Yin, X.M., and Dong, Z. (2017). Protein Kinase C δ Suppresses Autophagy to Induce Kidney Cell Apoptosis in Cisplatin Nephrotoxicity. *J. Am. Soc. Nephrol.* 28, 1131–1144.
38. Wang, P., Luo, M.L., Song, E., Zhou, Z., Ma, T., Wang, J., Jia, N., Wang, G., Nie, S., Liu, Y., and Hou, F. (2018). Long noncoding RNA *lnc-TSI* inhibits renal fibrogenesis by negatively regulating the TGF- β /Smad3 pathway. *Sci. Transl. Med.* 10, eaat2039.
39. Ge, Y., Wang, J., Wu, D., Zhou, Y., Qiu, S., Chen, J., Zhu, X., Xiang, X., Li, H., and Zhang, D. (2019). lncRNA NR_038323 Suppresses Renal Fibrosis in Diabetic Nephropathy by Targeting the miR-324-3p/DUSP1 Axis. *Mol. Ther. Nucleic Acids* 17, 741–753.
40. Wang, J., Li, H., Qiu, S., Dong, Z., Xiang, X., and Zhang, D. (2017). MBD2 upregulates miR-301a-5p to induce kidney cell apoptosis during vancomycin-induced AKI. *Cell Death Dis.* 8, e3120.
41. Yang, R., Xu, X., Li, H., Chen, J., Xiang, X., Dong, Z., and Zhang, D. (2017). p53 induces miR199a-3p to suppress SOCS7 for STAT3 activation and renal fibrosis in UUO. *Sci. Rep.* 7, 43409.
42. Peng, J., Li, X., Zhang, D., Chen, J.K., Su, Y., Smith, S.B., and Dong, Z. (2015). Hyperglycemia, p53, and mitochondrial pathway of apoptosis are involved in the susceptibility of diabetic models to ischemic acute kidney injury. *Kidney Int.* 87, 137–150.